Available online at www.sciencedirect.com

ScienceDirect

Journal of Ocean Engineering and Science xxx (xxxx) xxx

www.elsevier.com/locate/joes

Original Article

Generation of rogue waves at model scale

Bailey Groves, Nagi Abdussamie*

National Centre for Maritime Engineering and Hydrodynamics, Australian Maritime College, University of Tasmania, Launceston, Tasmania, Australia

Received 7 September 2018; received in revised form 9 February 2019; accepted 9 February 2019
Available online xxx

Abstract

The study of rogue waves is becoming increasingly important, as the offshore oil and gas, as well as renewable energy industries, expand. The unpredictability of such disastrous waves poses a significant risk to floating and fixed structures, making it necessary to develop methods capable of recreating rogue waves for model testing purposes. In this paper, an investigation into the useability of the NewWave theory, a theoretical formula for producing focused waves, was conducted in model test facilities with a wavemaker. The numerical modelling of rogue waves was performed using MATLAB codes developed to create several types of wave packets. The success of the numerical generation of design rogue waves was dependent on the number of wave components used during construction such that a suitable rogue wave ($H_{max}/H_s > 2.0$) could be created using 400 or more components. It was found that the NewWave technique could construct and physically generate design rogue waves within a close range of the predicted height provided the main wavemaker stroke was smooth enough (at around 0.8 s trough-crest for the tested model scale). The measured rogue waves were found to be complex; highly non-linear in amplitude with the behaviour of up to the 3rd order. Furthermore, it was observed that rogue waves, created based on a 100-year sea state, were very similar to the New Year Wave confirming that such extreme waves, approximately 25–27 m high at full scale, can indeed occur in severe sea states.

Keywords: Rogue waves; Numerical modelling; Design rogue waves; Model testing; New Year Wave.

1. Introduction

The terms ‘freak wave’ or ‘rogue wave’ are common among seafarers early as the 19th century as an explanation for damage or delay to transport. Described as extreme waves that dwarf the surrounding ocean conditions and often the vessel itself, these ‘monsters’ appear at random and cause incredible damage [1–3]. The nature of these waves is described as random and extremely rare, but the power they contain is unfathomable [4,5]. Despite accounts of such events from seafarers, rogue waves were thought to be a myth as there was never any firm evidence of such a phenomenon. The problem arises whether to account for rogue waves in marine structure design and if so, how to do so given the lack of knowledge in their generation [2,6].

However, on January 1st 1995, a rogue wave of 25.6 m impacted the Draupner offshore jacket platform in the North Sea [7] during which the significant wave height in the region was only 11–12 m. The Draupner platform had been installed with a down-pointing laser instrument, which was intended to aid in monitoring wave loads on the bucket foundation. The laser instrument accurately recorded the rogue wave, which is now known as the New Year Wave (NYW). The platform legs were considered to have no impact on the wave interactions below the structure, which gave greater credibility to the wave elevation recording. The impact zone received a minor damage and no personnel was outside during the event [7]. This event was the first physical recording of a rogue wave, which would lead to the research and development of design criteria and modelling.

The accepted criteria for a rogue wave occurrence is when a wave reaches over double the ratio between its current height and significant wave height for that region, $H_{max}/H_s > 2.0$ (maximum crest to trough wave height criterion) [2,8]. Alternatively, $C_{max}/H_s > 1.3$ (maximum crest criterion) can be used to classify an occurrence, usually taken from a 20 min sea elevation record as per DNV [8]. The NYW

* Corresponding author.
E-mail address: nagia@utas.edu.au (N. Abdussamie).

https://doi.org/10.1016/j.joes.2019.02.001

Abbreviations and notations

H_s	significant wave height (m)
A	wave amplitude (m)
$C_{\max}$	maximum crest height (m)
CV	coefficient of Variation (%)
d	water depth (m)
f	frequency (Hz)
FFT	Fast Fourier Transform
H_b	breaking wave height (m)
$H_{\max}$	maximum wave height (m)
k	wave number (1/m)
m	mean value (varied)
MTB	Model Test Basin
N	number of wave components
NYW	New Year Wave
S	spectral power (m^2 s)
t_f	focal time (s)
T_p	peak period (s)
Tr	transfer function (-)
WP	wave probe
x_f	focal location (m)
γ	peak shape parameter (-)
Δf	frequency interval (Hz)
ε	phase angle (rad)
η	wave elevation (m)
σ	standard deviation (varied)
ω	angular wave frequency (rad/s)

height was 25.6 m (trough-to-crest), while H_s was only 11.9 m; since $H_{\max}/H_s = 2.15 > 2.0$ the event was, by definition, a rogue wave. The force of the impact was not as extreme as to be expected from such a large wave [7]. The recorded crest height of 18.5 m above the MSL also satisfied the maximum crest criterion ($C_{\max}/H_s = 1.55 > 1.3$). The weather conditions around the region were quite rough at the time, with at least two low-pressure systems located in Southern Sweden and around the southern areas of the North Sea. High winds were being generated all through the North and Norwegian seas, however, the Draupner platform was located just outside the boundary of most extreme winds [7]. The various pressure differentials around the region due to extreme weather would have caused significant swell, leading to two sources of waves propagating past the Draupner installation; wind-driven and swell.

The actual cause of the NYW is still unknown to date, and only theories relating to rogue waves, in general, are possible explanations [9–12]. The 100-year return period storm design wave height was estimated at around 27 m and was evidently larger than the recorded rogue wave. The 10,000-year return period storm maximum crest height was predicted at around 19.5 m, which was once again, greater than the 18.5 m rogue wave crest experienced. The NYW data has since been extensively analysed for understanding its cause and how it could relate to general rogue wave mechanics and applicability to design/operation rules. There are five potential mechanisms hypothesised; dispersive focusing, spatial focusing, non-linear focusing, superposition and wave crossing [13]. The accepted method among these techniques is that wave groups focusing at a given location result in an extreme peak of energy and height beyond short-term predictions [2].

- Superposition theory is the most basic method in which individual waves of random frequencies and phases will eventually match the phase and construct a rogue wave. Ning et al. [14] conducted focused wave experiments using the superposition theory, and results showed that the desired creation of the theoretical signal was dependent on the phase angle of each component. It was also found that non-linear interactions governed the wave structure more strongly at increased steepness, with steeper waves deviating from non-linear predictions. However, questions the statistical relevance of random linear superposition, as the occurrence chance is very high. Compared to actual rogue wave statistics, superposition of linear waves is in many cases improbable of occurring [15].
- Dispersive focusing is like superposition in that it relies on wave packets to focus into an extreme wave at a specific location and time. Dispersive waves show strong focusing potential even with random phases, however, the replicability in ocean environments is questionable since it is not believed such focusing requirements can be produced [13].
- Spatial focusing depends on geographical properties of the ocean as well as currents to cause alignment of waves, such as areas that create refractions or reflections. This method, however, does not provide the reason as to how alignments can occur in deep water, where the necessary spatial focusing factors may not be present.
- Non-linear focusing is based on the amplification effects of modulation instability, where non-linear behaviours can deviate from wave motions into random extreme events [16]. Theories like Non-linear Schrodinger solutions (NLS) and the Akhmediev–Peregrine extension are examples of such focusing methods [17,18]. Although theoretically viable, real world ocean conditions allow for directional spreading of energy while the mathematical solution assumes unidirectional energy motion [19].
- Wave crossing is the ability for two unidirectional wave groups to eventually create a very large wave peak. Such a theory is more realistic in that most ocean conditions are directionally spread, hence would be more accurately modelled using a crossing sea. Other rogue wave methods require following seas (unidirectional). Analysis into the Draupner incident by Adcock et al. [15] showed that such a wave would break under a following sea using the standard second order theory. However, it would maintain its structure if analysed using bidirectional seas at a large angle to each other, with fully non-linear modelling.

A common method of creating rogue waves numerically is the NewWave formula, which is an accepted method based on superposition theory. The scope of this paper is to investigate

Please cite this article as: B. Groves and N. Abdussamie, Generation of rogue waves at model scale, Journal of Ocean Engineering and Science, https://doi.org/10.1016/j.joes.2019.02.001

the useability of the NewWave formula in generating design rogue waves both numerically and physically. Such design waves were required to appear suddenly amidst a standard irregular sea state to accurately simulate how real-world rogue waves have occurred in the past. The accuracy of experimental rogue wave heights and the contained energy compared to the numerical models were studied using time-domain and spectral analyses. To compare the design wave models with an actual recorded rogue wave event, the rouge waves created by the NewWave theory were compared with the Draupner NYW.

2. NewWave theory

The NewWave formula is derived from superposition focusing methods, shown below [14]:

$$\eta(x,t) = \sum_{n=0}^{N} a_n \cos\left(k_n(x - x_f) - \omega_n(t - t_f) + \varepsilon_n\right) \quad (1)$$

where the wave elevation η is a function of the component amplitude a_n, wave number k_n, angular frequency ω_n, and the relative phase angle ε_n. The target time and position t_f and x_f, respectively enable the original time series data to be altered, resulting in a phase shift to move the rogue wave occurrence as desired. The signal is constructed using multiple wave components N that are summed at each time step; hence the solution is essentially a magnitude of linear wave signals being forced together into a random combination. Previous work by Banks and Abdussamie [20] showed that the creation of focused waves using the NewWave formula was heavily dependent on the input phase angle ε_n. A method for approximating each component amplitude a_n based on a generic spectrum is expressed as;

$$a_n = \sqrt{2S(f_n)\Delta f} \quad (2)$$

where $S(f_n)$ is the total energy at the component frequency f_n, and Δf is the frequency interval.

The simulation of rogue waves was performed using MATLAB codes developed to create several types of wave signal programs. Fast Fourier Transform (FFT) was required to interpret preliminary experimental results. Microsoft Excel was also used, taking information directly exported from MATLAB, to create wavemaker seas state files for later physical experimentation. The models were tested experimentally in a wave basin facility after being developed and analysed numerically, with the procedure detailed below in Fig. 1.

The design simulation model was built upon Eq. (1) and incorporated with an input for user-defined significant wave height and period (H_s and T_p) to form a base sea state i.e. JONSWAP spectrum. The developed model was designed such that it could automatically iterate random irregular wave signals until a rogue wave had been generated, by assigning random phases ε_n at every iteration. The criteria for a successful rogue wave was set as $H_{max}/H_s > 2.0$ within the numerical code, which was implemented via a wave height check function in MATLAB codes. The model factored water depth into Eq. (1) when solving the component wave number k_n, however, this proved obsolete as x_f was always set to 0.0 m during simulation. The frequency bandwidth (the number of wave components) was also user specified. The time step was set to 0.10 s to provide a smooth wave signal including the rogue wave peak. The effect of the component number on generating a successful rogue wave was investigated, with the testing method outlined in Table 1. The results of numerical rogue waves generated if the design rogue wave model was successful would be validated through model-scale testing.

Table 1
Numerical wave tests.

Test	Wave components
Test 1	50
Test 2	100
Test 3	500
Test 4	1000

Table 2
Sea state input parameters for JONSWAP spectrum.

Sea state	Full-scale		Model-scale (1:100)		γ
	H_S (m)	T_p (s)	H_S (m)	T_p (s)	
Sea 1	11.900	17.00	0.119	1.700	3.3
Sea 2	12.700	14.100	0.127	1.410	3.3

Eq. (1) was modified to include the wavemaker transfer function (Eq. (3)), for experimental testing of the design wave model as;

$$S(t) = \sum_{n=0}^{N} \frac{a_n}{Tr_n} \cos\left(k_n(x - x_f) - \omega_n(t - t_f) + \varepsilon_n\right) \quad (3)$$

The transfer function for a piston-type wavemaker is shown below [21];

$$Tr_n = \frac{2\cosh(2k_n d) - 1}{\sinh(2k_n d) + 2k_n d} \quad (4)$$

where d is the water depth and k_n is the wave number.

3. Test matrix

Two sea states were selected for this investigation as represented by the JONSWAP spectrum which was formulated as a modification of the Pierson–Moskowitz spectrum for a developing sea state in a fetch limited situation (Table 2). An average value ($\gamma = 3.3$) was selected for the peak shape parameter [8]. Both sea states were an attempt to model a rogue wave in similar conditions to the Draupner site in 1995 [7,15]. The model scale JONSWAP spectrums for both sea states are shown in Fig. 2. Several 30 min full-scale sea elevation time series were created in MATLAB and then scaled down using Froude's law at 1:100 scale. The scaled time series that contained a rogue wave was finally trimmed to 11–14 s with some of an irregular wave train left in after the target wave to simulate a more realistic sea in a physical tank. It should be

Please cite this article as: B. Groves and N. Abdussamie, Generation of rogue waves at model scale, Journal of Ocean Engineering and Science, https://doi.org/10.1016/j.joes.2019.02.001

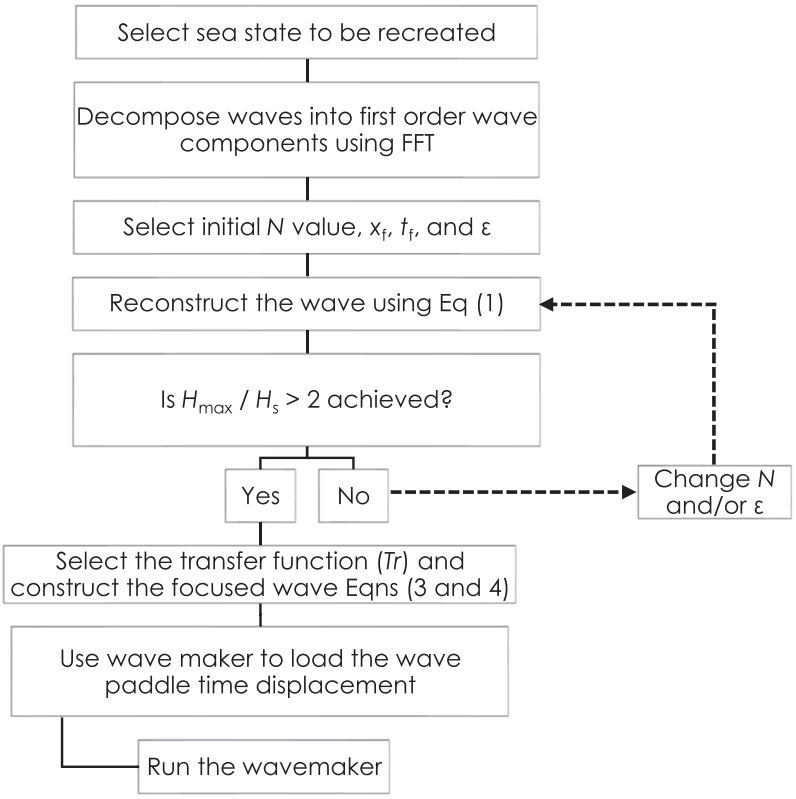

Fig. 1. Testing procedure flowchart for creating rouge waves in a physical wave tank.

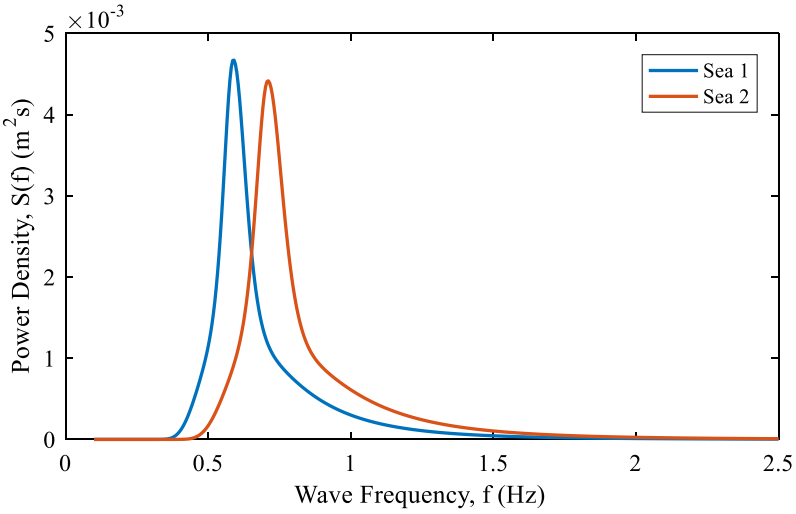

Fig. 2. JONSWAP spectrum for sea states 1 and 2 at model scale.

stressed that such a short-time window would allow for testing in the physical tank without interference from reflected waves travelling back up the tank [14,20].

4. Experimental testing

4.1. Set-up

The physical modelling of rogue waves was performed in the Australian Maritime College's Model Test Basin (MTB) facility. The experimental setup is shown in Fig. 3. The basin is 35 m long x 12 m wide. The water depth used throughout the experiment was tested twice at 0.6 m and 0.7 corresponding to 60 m and 70 m at full-scale which approximately matched the full-scale mean water depth at the Draupner site (60–70 m) [15]. A 16-paddle piston-type wavemaker was situated at one end of the basin, perpendicular to the length, with an artificial beach located at the other end. The beach was comprised of stiff foam blocks to dissipate large amounts of wave energy. To record the passing rogue waves, conductor

Please cite this article as: B. Groves and N. Abdussamie, Generation of rogue waves at model scale, Journal of Ocean Engineering and Science, https://doi.org/10.1016/j.joes.2019.02.001

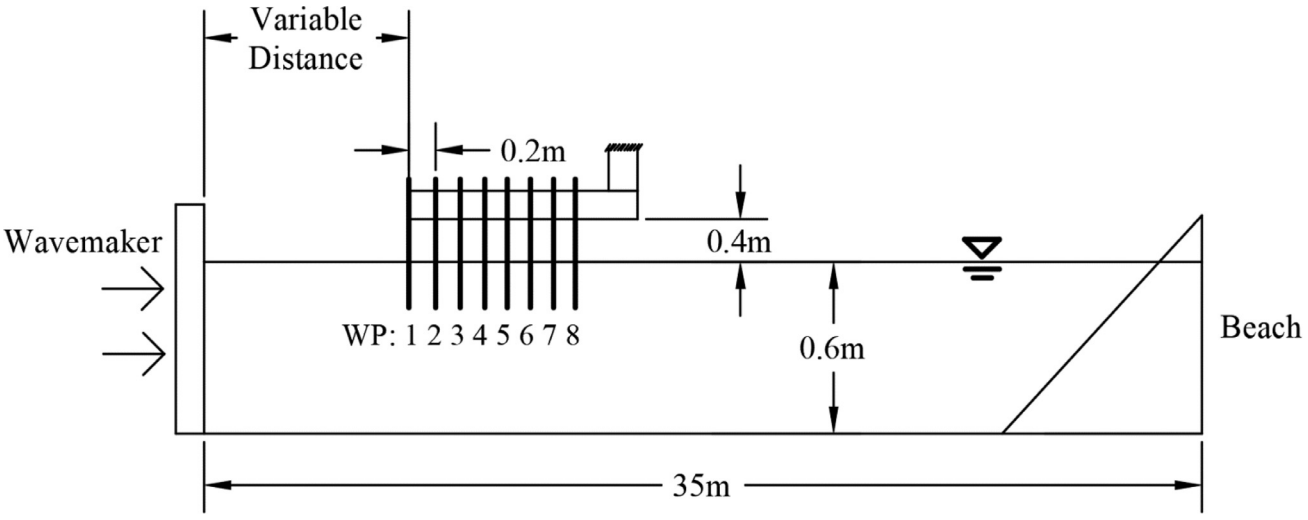

Fig. 3. Profile view (xz plane) of experimental setup [not to scale].

type wave probes were used with a sampling frequency of 20 Hz, arranged in an array at the longitudinal centreline of the tank and parallel to the wave direction to capture the wave propagation. A total of 8 wave probes, spaced 0.20 m apart, were suspended off a towing carriage above the water. Such a test rig was to allow both a longitudinal placement of the probe array to optimise the focal point, and to avoid disturbing the water. The variable distance between the wavemaker paddles and the first wave probe was due to the uncertainty of where the rogue waves would focus and was examined based on trial and error during wave calibration.

The wavemaker was operated in "externally generated seas" which allowed for direct control over the wave signal created, using paddle displacement ".prn" space delimited text files. The wave signals created in MATLAB were passed through a wavemaker transfer function, which converts the water elevation at each time step to a paddle displacement.

To prevent any damage to the wavemaker drive system during start-up, around 2 s of ramping was added to the beginning of the stroke time series record; the ramp was a sinusoidal function with increasing amplitude. The allowable ramping amplitude was limited to less than the initial stroke amplitude of the wave signal to avoid transfer of excessive energy into the water before the design waves were generated.

4.2. Data analysis

It is worth mentioning that the 1:100 model scale of the experiment reaches the acceptable limit in hydrodynamic model testing [8]. The presence of small-scale hydrodynamic flow instability and turbulence might therefore have a role in the observed variability in the measurements of rogue waves. The uncertainty of the measured rogue waves in both time and magnitude was estimated by running several (up to three) repeats for each wave condition and assessing the variability of the results for the waves. Referring to Fig. 4 the time series data is shown for the leading and trailing wave probes (WP1 and WP8). It is seen that, the relationship between the wave heights is almost constant and highly repeatable except at the wave crest (denoted by C_{max}). Table 3 presents the data variation assessment using the standard deviation (σ) and the coefficient of variation ($CV = \sigma/m$ where m is the mean value) with respect to the measured peak focal wave (C_{max}). The obtained values for CV were within 5% for all wave probes (WP1 – 8) further providing confidence in the experimental repeatability. These findings were also supported by a previous work [20,22] conducted at a smaller scale (1:125) which has indicated that good qualitative repeatability can be found among multiple repeated runs for all wave probes used in their model tests such that lower values of CV were obtained during the calibration of generated waves.

Table 3
Results of uncertainty analyses for maximum crest height (C_{max} in meter).

WP	1	2	3	4	5	6	7	8
Run 1	0.180	0.150	0.168	0.167	0.166	0.164	0.155	0.165
Run 2	0.165	0.162	0.164	0.164	0.169	0.163	0.170	0.166
Run 3	0.182	0.164	0.169	0.166	0.166	0.171	0.166	0.170
Mean, m	0.176	0.159	0.167	0.165	0.167	0.166	0.164	0.167
Std. dev., σ	0.010	0.008	0.003	0.001	0.002	0.004	0.008	0.002
CV	5%	5%	2%	1%	1%	3%	5%	1%

5. Results and discussion

5.1. Numerical results

The model scale results of numerical generation of rogue waves are shown in Fig. 5 for the numerical tests listed in Table 1. Overall, the numerical design rogue wave program developed was successful in generating rogue waves using the NewWave theory. The number of wave components used to construct each wave affected how many phase iterations were required to successfully create a rogue wave satisfying the criterion $H_{max}/H_s > 2.0$. Below 100 components, wave signals

Please cite this article as: B. Groves and N. Abdussamie, Generation of rogue waves at model scale, Journal of Ocean Engineering and Science, https://doi.org/10.1016/j.joes.2019.02.001

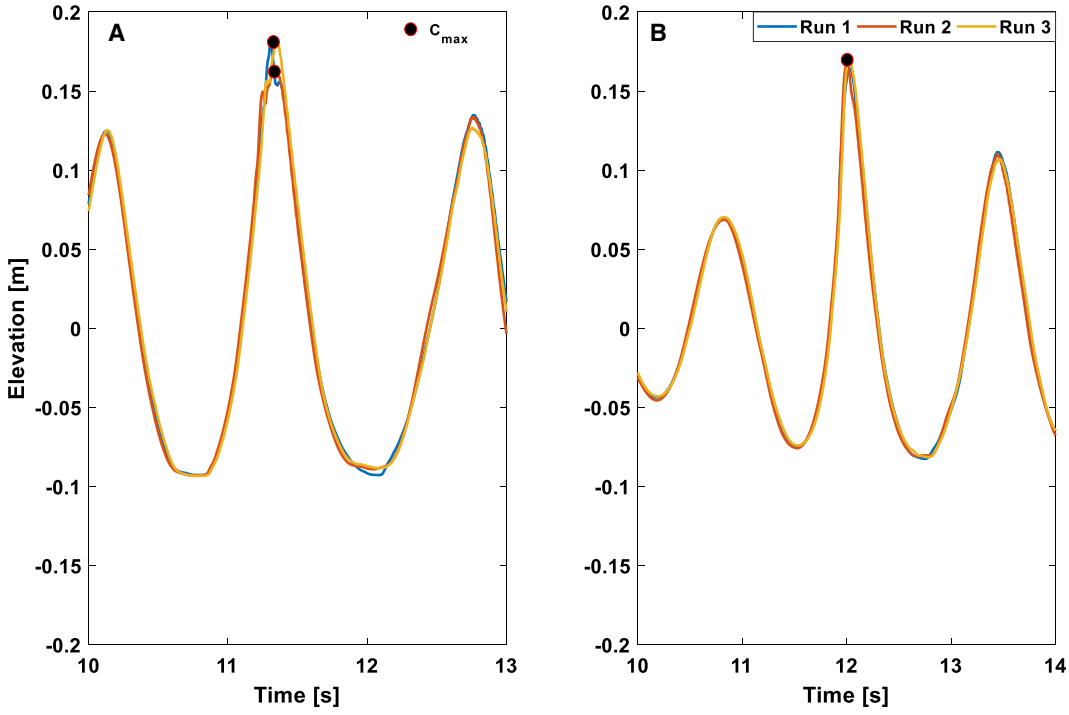

Fig. 4. Time history of rogue waves for three repeated runs at WP1 (A) and WP8 (B).

appeared to repeat several times over the 180 s time window (30 min at full scale) due to the limited number of random phase angles, and the chances of generating a rogue wave were incredibly low. It was found that increasing the number of components ($\geq$ 400 components) improved the chances; a secondary effect observed was that the wave signal was more irregular and realistic over the tested time window. However, this improvement did not extend beyond 500 components, as up to 1000 appeared to decrease the chances of a successful rogue wave.

The signals in Fig. 5(C) and (D) for tests 3 and 4 appear to simulate rogue wave occurrences like the NYW observed at the Draupner site [7] such that the extreme wave occurred suddenly within a sea state modelling the design conditions [12,23]. Test 3 achieved $H_{max}/H_s = 2.13$, and test 4 achieved $H_{max}/H_s = 2.28$. It was found that some rogue waves occurred as a large peak followed by an extreme trough (such as test 4), rather than simply a very large peak with shallow trough (i.e. the NYW). Such a behaviour was likely due to the water depth not affecting the component wave signals in Eq. (1), as the position variables x and x_f were 0.0 m, which resulted in the wave number also equal zero. Since k_n had been removed, wavelength and hence the effect of water depth had also been removed.

The corresponding spectral analysis for tests 1–4 is shown in Fig. 6 in which good agreement between the original JONSWAP and recorded spectrums can be seen. In all tests, the irregular sea state generated closely matched the JONSWAP spectrum, with minor deviations at peak and higher bandwidth frequencies. However, there is a noticeable difference in test 3 and 4 where successful rogue waves were contained in the sea state (Fig. 5); there is a secondary energy peak at higher frequencies between 0.7 and 0.9 Hz. These peaks are evidence of how deviated the rogue waves are from the rest of the irregular sea state. The design rogue wave model, with 400–500 wave components, was deemed successful at generating irregular sea states matching a base JONSWAP that also contained a random rogue wave. Due to this success, numerical rogue waves were physically modelled, with the main desire to observe the non-linear effects and the influence of water depth.

5.2. Experimental results

Fig. 7 shows the time history of wave elevations of the array of wave probes (WP1 – WP8) for sea states 1 and 2. Of notice the phase shift among wave probes, as the data was recorded in a single time reference. For sea state 1, the leading wave probe (WP1) appeared to record slightly more extreme crest elevations building up into the rogue wave. Meanwhile, the measured waves seemed to reach the steady state along the succeeding wave probes WP2 – WP8 for both sea states. Such findings were also confirmed by referring to the FFT results shown in Fig. 8 which indicated that there is a higher energy in the leading probes at the peak frequency, and the wave energy propagation along the 1.40 m array recorded by each probe had similar spectral energy levels and trends, with slight reductions in sequential probes. Through trial and error, it was found that the leading wave probe (WP1) and the trailing wave probe (WP8) had to be placed 2.5 m and 3.9 m, respectively, away from the wavemaker paddles. This position was used for all tests of the design rogue wave model.

Please cite this article as: B. Groves and N. Abdussamie, Generation of rogue waves at model scale, Journal of Ocean Engineering and Science, https://doi.org/10.1016/j.joes.2019.02.001

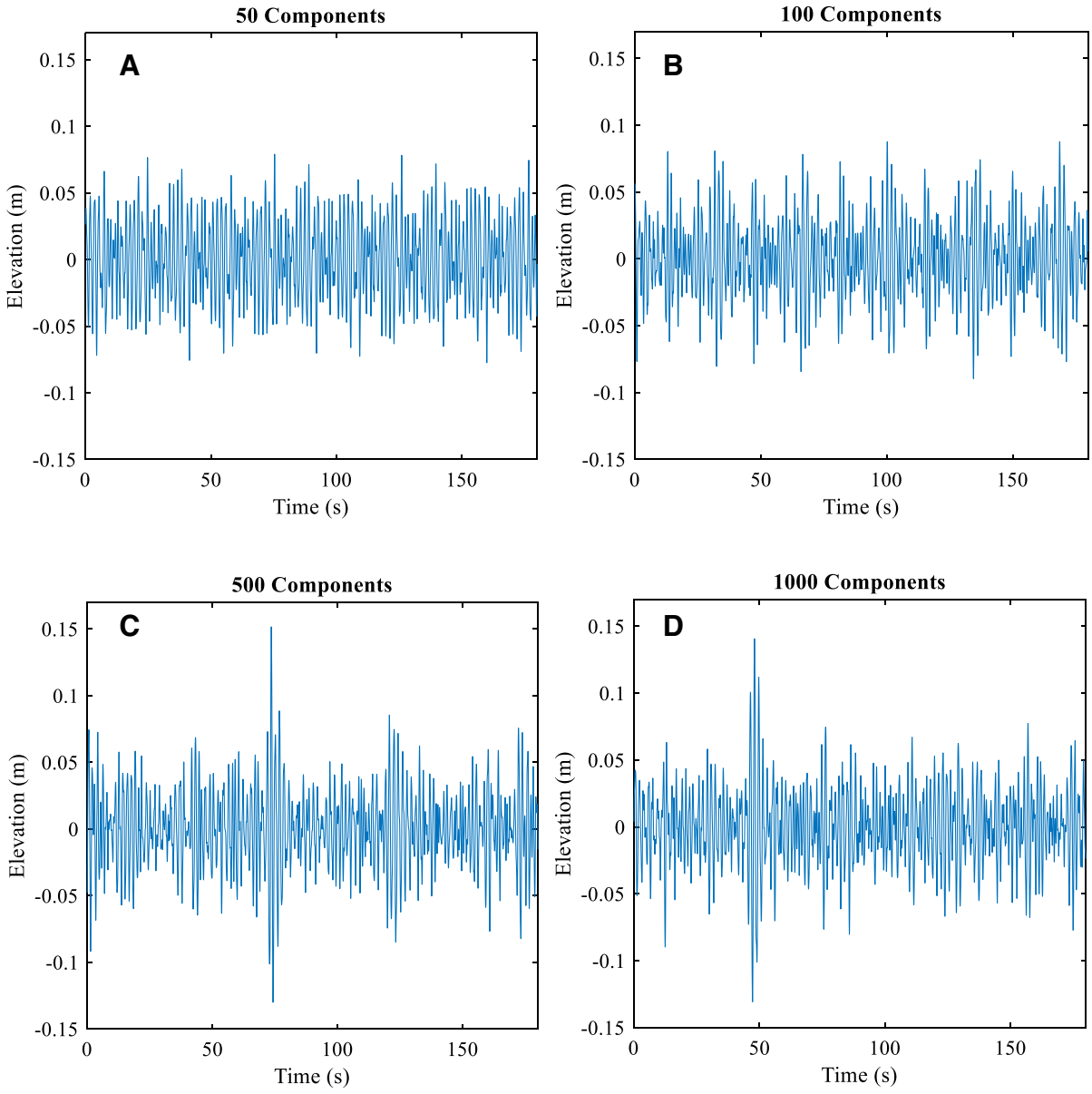

Fig. 5. Theoretical wave elevations using different wave components for sea state 1: test 1 (A), test 2 (B), test 3 (C) and test 4 (D).

Since the obtained wave data were quite consistent along the 8 WPs, particularly for sea state 2, the data of the leading wave probe (WP1) was used to validate the numerical models for the analysis and results discussed hereafter.

5.3. Comparison of experimental and numerical results

Figs. 9 and 10 show the time history of rogue waves generated based on sea states 1 and 2. Two repeated runs per each sea state were used to observe the repeatability of rogue waves and to validate the numerical models. Both runs appear to be almost identical for both sea state 1 and 2 indicating the repeatability of such methods. Overall, model testing showed good agreement between the measured and numerical target wave crest heights, with significant non-linearity in the physical wave. Table 4 presents a comparison between the theoretically and experimentally generated rogue waves measured at WP1. The measured maximum wave heights were typically 0.4–2.7% lower than the desired target height, with one test deviating to 5.15% below the predicted elevation, however, these ranges are acceptable given $H_{max}/H_s > 2.0$ was still achieved. The maximum crest height criterion $C_{max}/H_s > 1.3$ was also achieved by all test runs. The experimental error was analysed at the focused wave point where the largest wave height occurred in each test with run 2 (sea state 2) having the largest error of 5.15% and run 1 (sea state 2) having the lowest error of 0.37%. There was one run (sea state 2) that exceeded the predicted value by 0.37%. Fig. 10 (sea state 2) shows more deviation between the target and measured waves such that both runs exhibit a significant non-linearity around the target rogue wave. These non-linear wave motions are seen in the troughs/crests before and after the extreme wave

Please cite this article as: B. Groves and N. Abdussamie, Generation of rogue waves at model scale, Journal of Ocean Engineering and Science, https://doi.org/10.1016/j.joes.2019.02.001

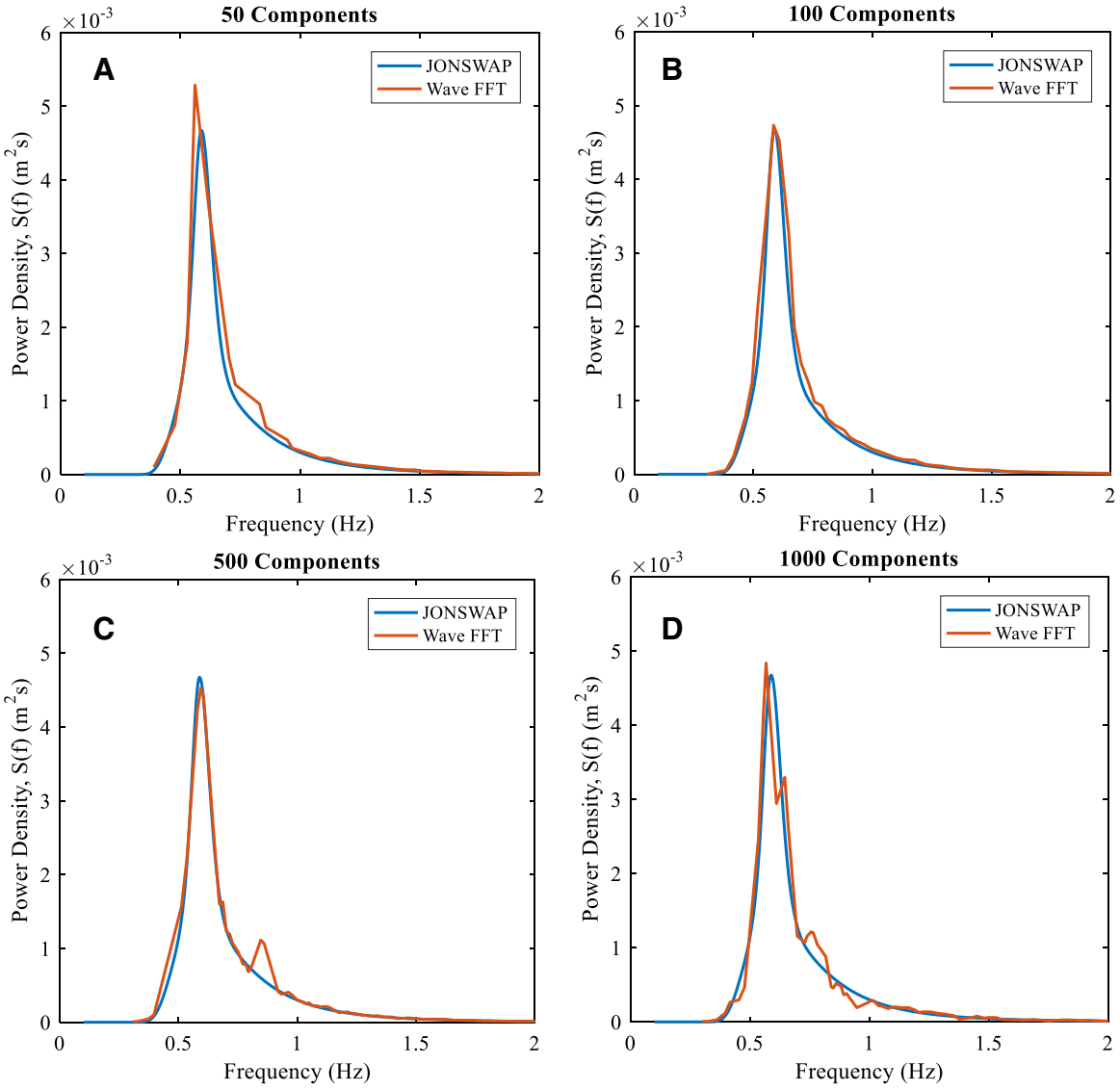

Fig. 6. FFT results of wave elevations compared with JONSWAP spectrum for test 1 (A), test 2 (B), test 3 (C) and test 4 (D).

Table 4
Rogue wave results.

Sea state	Target H_{max} (m)	Measured H_{max} (m)		H_{max}/H_s		H_{max} difference (%)	
		Run 1	Run 2	Run 1	Run 2	Run 1	Run 2
Sea 1	0.258	0.251	0.256	2.109	2.151	−2.713	−0.775
Sea 2	0.272	0.273	0.258	2.150	2.032	0.368	−5.147

occurrence. This behaviour indicates that the numerical design wave model does not factor water depth correctly, as the measured rogue waves are being forced "upwards" beyond predicted elevations.

The spectral analysis of experimental waves at WP1 compared to the design model is shown below in Fig. 11. The recorded spectral plots showed a similar trend and peak frequency for both sea states, albeit the power density recorded was less than estimated by the numerical design FFT such that the measured waves were less energetic than the design models at their main peak frequencies, which coincides with the observed reduction in wave heights. The overall recorded spectrum, however, peaks and trends were almost identical to the numerical one; the main spike with a minor secondary peak at a higher frequency. The peak power density and frequency of each sea state was higher than the design JONSWAP spectrum used (Fig. 2), but the difference between the two sea states was similar. The numerical design wave spectrum of sea state 1 (Fig. 11(A)) peaked at 0.59 Hz and sea state (Fig. 11(B)) peaked at 0.71 Hz, both of which are the

Please cite this article as: B. Groves and N. Abdussamie, Generation of rogue waves at model scale, Journal of Ocean Engineering and Science, https://doi.org/10.1016/j.joes.2019.02.001

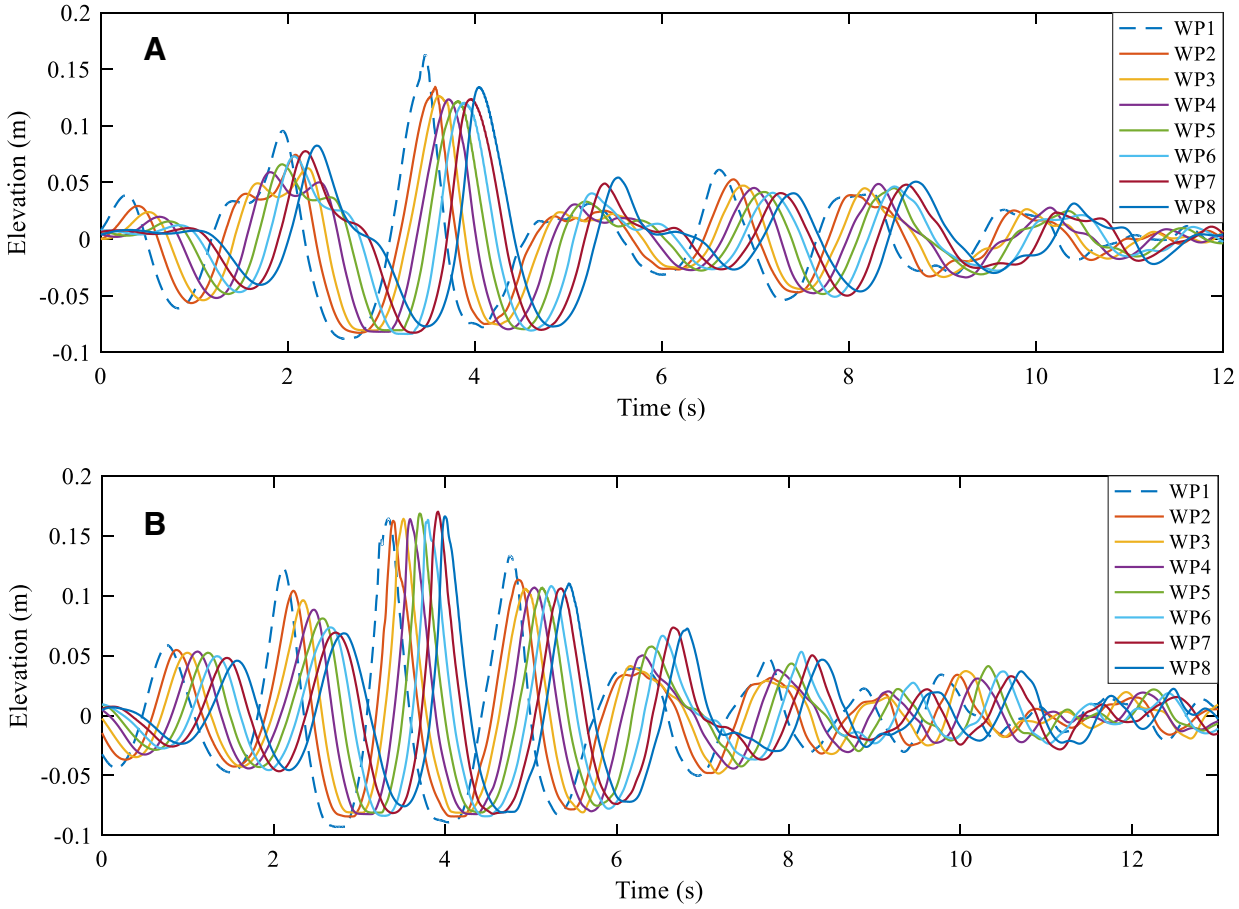

Fig. 7. Time series results of measured rogue waves at WP1-WP8 for sea state 1 (A) and sea state 2 (B).

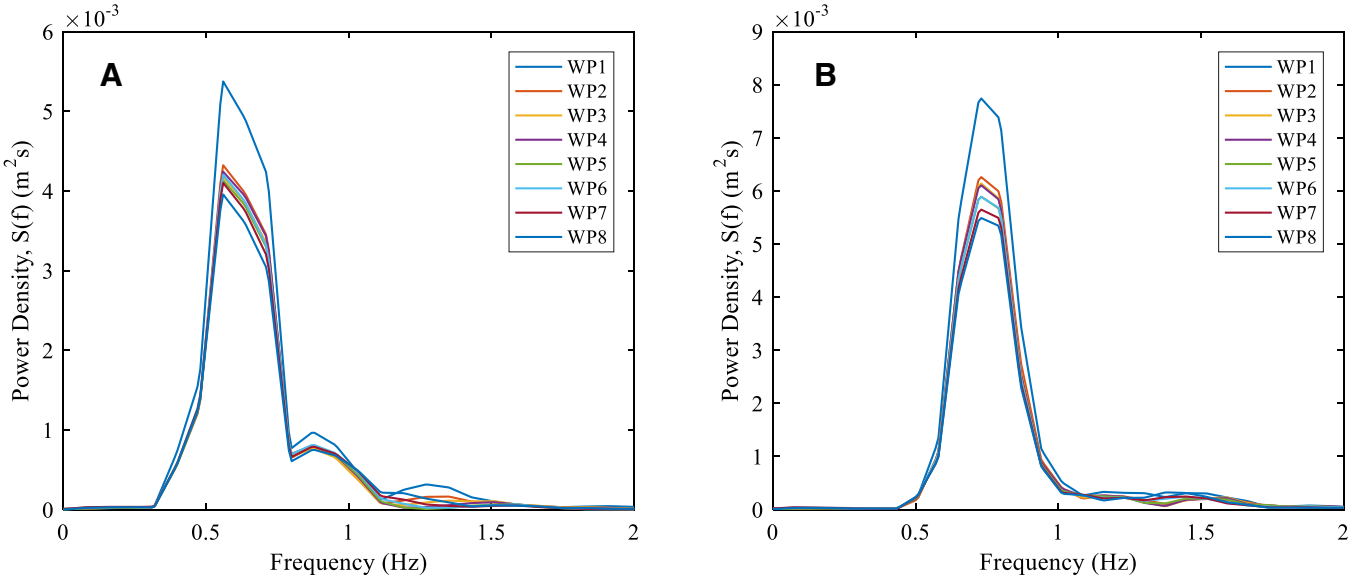

Fig. 8. FFT results of measured rogue waves at WP1-WP8 for sea state 1 (A) and sea state 2 (B).

same as their base JONSWAP plots, respectively. Sea state 1 recorded a peak energy of 0.0054 m^2s which was 17.4% more than its original JONSWAP, and sea state 2 measured 0.0079 m^2s which was 79.6% greater compared to its JONSWAP original [8]. The increase in recorded power density is due to the wave signal containing mostly the rogue wave signal and little of the normal irregular sea state (H_s), leading to FFT returning a very energetic sample. Testing with additional signal time before and after the rogue wave would bring the spectrums closer to their original JONSWAP design sea state.

Please cite this article as: B. Groves and N. Abdussamie, Generation of rogue waves at model scale, Journal of Ocean Engineering and Science, https://doi.org/10.1016/j.joes.2019.02.001

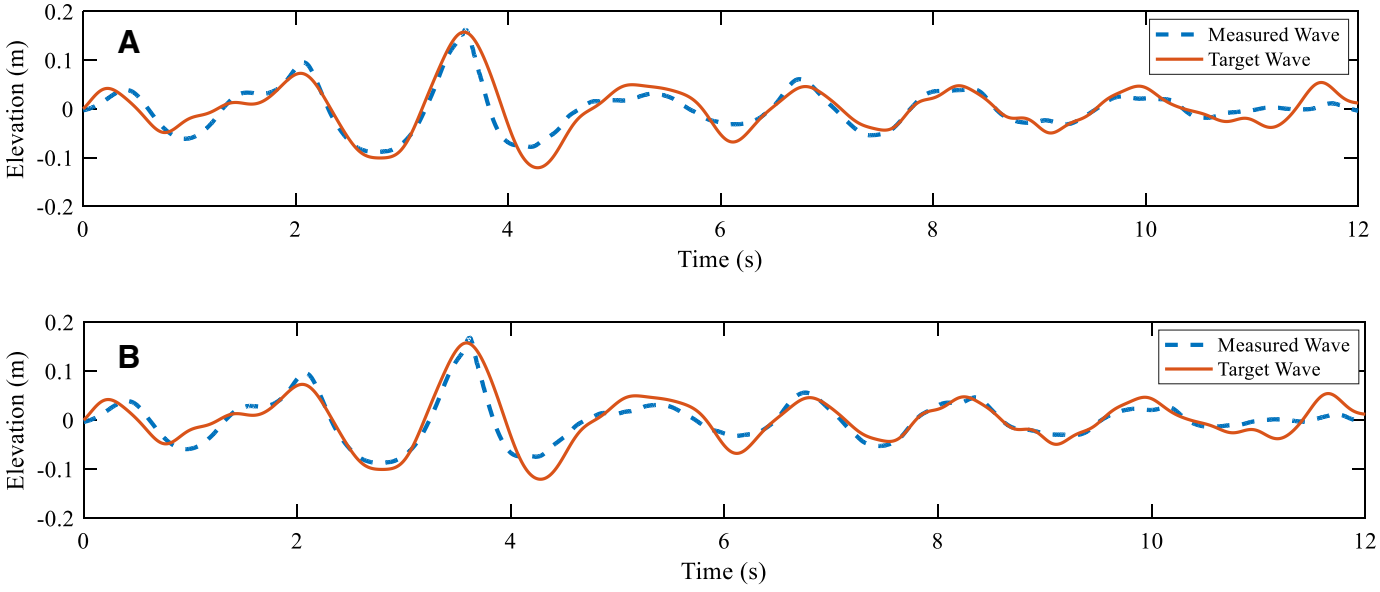

Fig. 9. Time series of measured and theoretical rogue wave elevations for sea state 1 using run 1 (A) and run 2 (B).

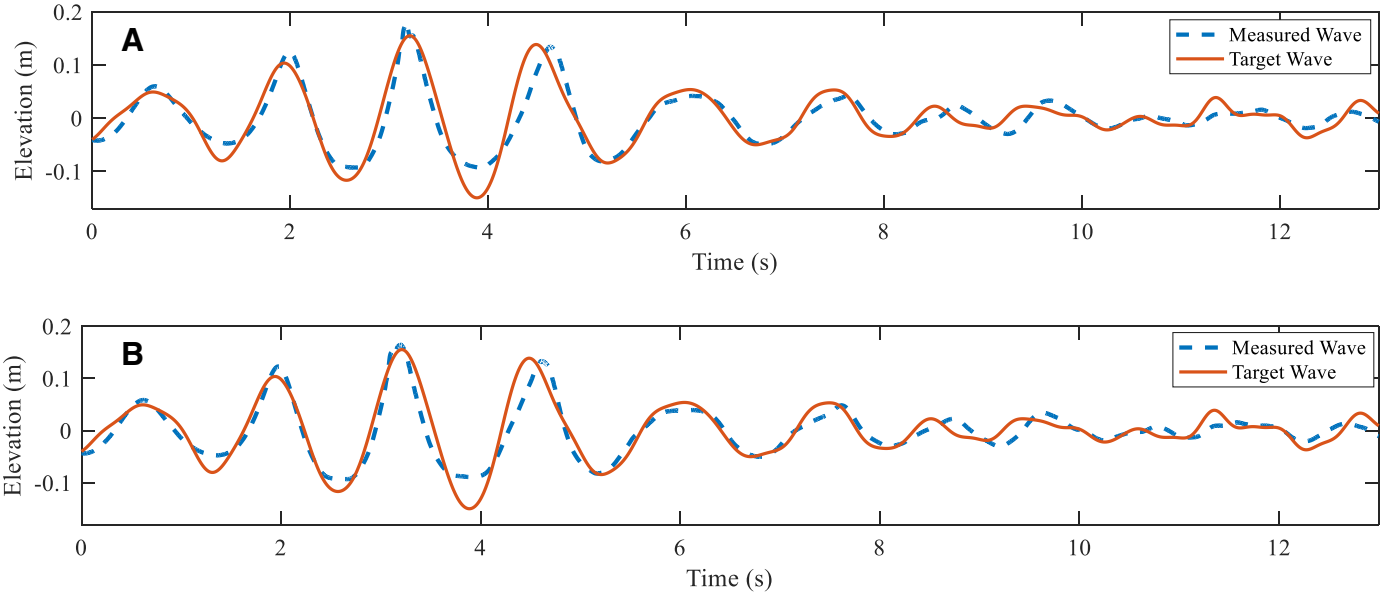

Fig. 10. Time series of measured and theoretical rogue wave elevations for sea state 2 using run 1 (A) and run 2 (B).

Table 5
Properties of tested rogue waves.

Sea state	H/gT^2 (-)	d/gT^2 (-)	H_b (m)	Wave condition	Order
Sea 1	0.012	0.029	0.362	Intermediate	Stokes 3rd
Sea 2	0.015	0.034	0.297	Intermediate	Stokes 3rd

Based on the wave parameters, the generated rogue waves are constructed with non-linear Stokes mechanics up to the 3rd order using the recommended methods of DNV [8]. Additional properties of the measured rogue waves are shown in Table 5 in which H_b is the breaking wave height limit. This coincides with similar rogue wave experimentation by Deng et al. [24] where tank generated freak waves closely modelled numerical Stokes 3rd Order waves. Observations during testing, the waves passing WP1 were unstable at the crest and are believed to have been breaking at this location. However, both rogue waves were below the breaker height limit; wave-wave interactions could have led to some instability and resulted in the rogue wave crests breaking while still maintaining most of their height and energy. Despite the minor crest breakers, the tested design waves reached the target heights and satisfied rogue wave criteria, hence the waves are considered a success. The results discussed proved the authenticity of experimental rogue waves despite the visual deviations in the presented figures, which showed overestimated trough depths. These

Please cite this article as: B. Groves and N. Abdussamie, Generation of rogue waves at model scale, Journal of Ocean Engineering and Science, https://doi.org/10.1016/j.joes.2019.02.001

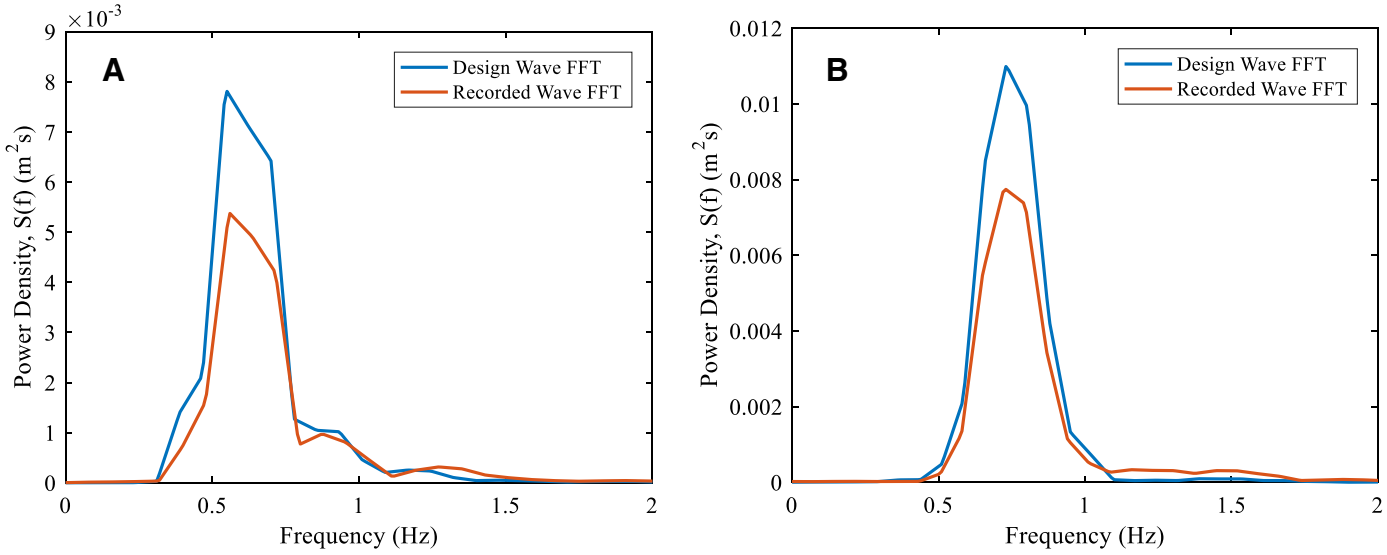

Fig. 11. FFT results of measured and target rogue waves at WP1 for sea state 1 (A) and sea state 2 (B).

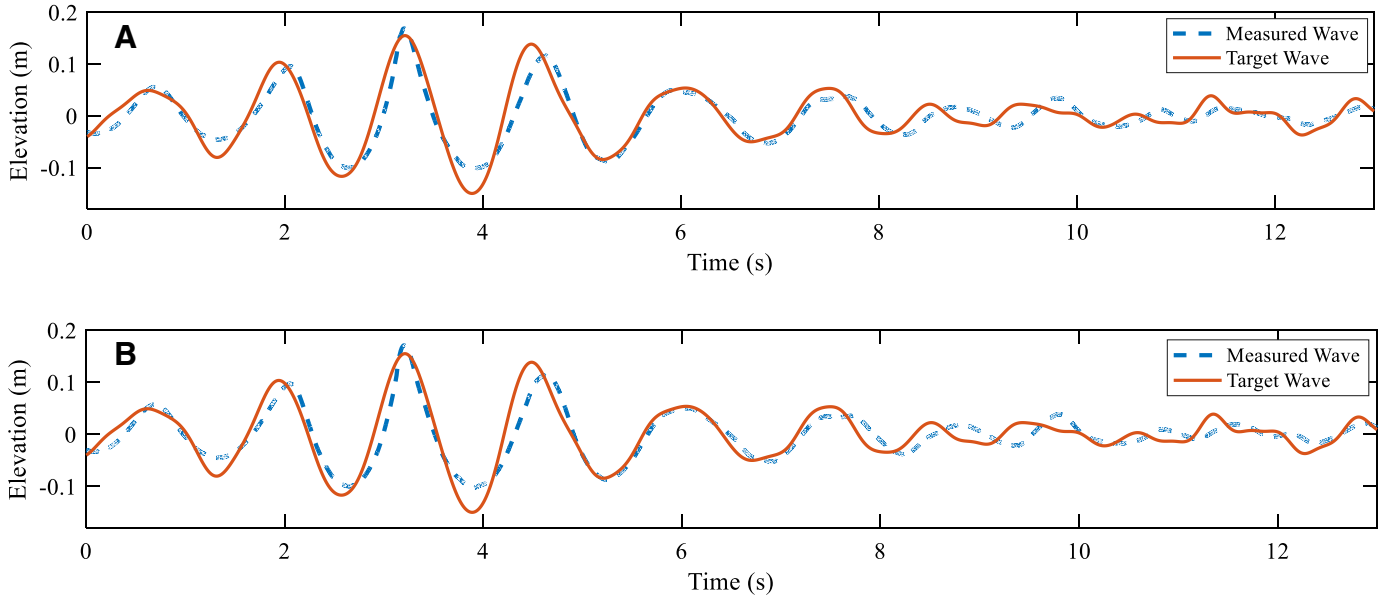

Fig. 12. Time series of measured and theoretical rogue wave elevations for sea state 2 in water depth = 0.7 m for run 1 (A) and run 2 (B).

results are likely due to the rather shallow water depths causing highly non-linear behaviour in the experimental waves.

5.4. The influence of water depth

A Water depth of 0.7 m was also tested to ascertain any change in wave heights. Overall, an increase of 0.1 m in the water depth was found to reduce the non-linearity of the generated rogue wave. By comparing Figs. 10 and 12, the crest heights at $d = 0.7$ m appeared to be similar to the one measured at 0.6 m depth, but the troughs before and after the main target crest are deeper. The troughs in Fig. 12 also appear to be less flat, compared to Fig. 10, which suggests that the extra 0.1 m depth had a significant role in the shallow water behaviour of the experimental rogue waves.

The measured wave heights and rogue wave criterion results are presented in Table 6. Comparing the measured wave heights to the target waves, there is clear agreement on the trough-crest elevation achieved by the experimental testing, particularly at deeper conditions. Every test conducted was able to generate a rogue wave of $H_{max}/H_s > 2.0$ based on the original design significant wave height, proving the success of the numerical design models.

5.5. Comparison of observed waves and the Draupner NYW

Inspecting the results of sea state 1, the generated rogue wave was found to be quite similar to the Draupner NYW

Please cite this article as: B. Groves and N. Abdussamie, Generation of rogue waves at model scale, Journal of Ocean Engineering and Science, https://doi.org/10.1016/j.joes.2019.02.001

Table 6
Rogue wave results for sea state 2 at different water depths.

Water depth (m)	Target H_{max} (m)	Measured H_{max} (m)		H_{max}/H_s		H_{max} difference (%)	
		Run 1	Run 2	Run 1	Run 2	Run 1	Run 2
0.6	0.272	0.273	0.258	2.150	2.032	0.368	−5.147
0.7	0.272	0.270	0.271	2.126	2.134	−0.735	−0.368

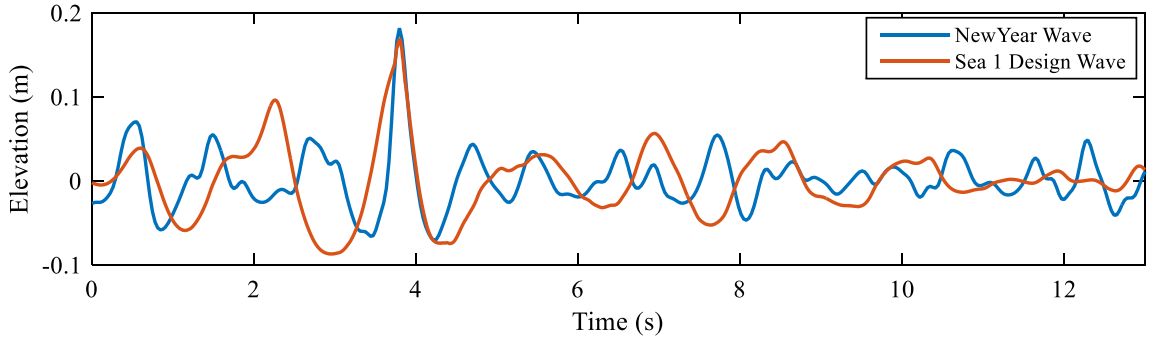

Fig. 13. Time series of observed rogue wave for sea state 1 compared with the Draupner NYW at 1:100 scale.

(Fig. 13). The rogue wave observed in the basin had almost identical slopes after the main crest peak and the signal returns to a normal irregular sea state after the occurrence of rogue wave, however, the leading slope of the design wave is much less steep than the NYW (the same behaviour was observed for sea state 2). This difference in leading slopes between signals is due to the design wave test being unidirectional. Adcock et al. [15] stated that numerical unidirectional signals identical to the NYW would break before reaching the target height, therefore the design rogue wave was likely successful because it had a less steep leading slope, so the period was larger. Such an observation indicated that rogue waves, created based on a 100-year sea state, were very similar to the New Year Wave confirming that such extreme waves, approximately 25–27 m high at full scale, can indeed occur in severe sea states.

6. Conclusions

This paper presented results of a numerical and experimental study of rogue waves generated at a model scale of 1:100. The numerical design rogue wave model was established to test the effect of the component number when utilising the NewWave technique to construct wave signals with random phases. Based on the results presented in this paper, the following conclusions were drawn:

1. It was found that 100 wave components or less could not numerically generate a suitable rogue wave ($H_{\max}/H_s > 2.0$), with the design model requiring around 400 or more components to be successful.
2. Rogue waves could be successfully recreated in a wave basin if the wavemaker stroke had a large period from the trough to crest of its motion (at around 0.8 s trough-crest for the tested model scale), otherwise, the forced water column tended to break immediately and dissipate energy through the basin. The design rogue wave model was successful in outputting wavemaker displacements which could be recreated signals that were in good agreement to their original numerical models, albeit more non-linear in particle motions which could be attributed to the limited water depth tested.
3. It was observed that the wave troughs of rogue waves were predicted much deeper in the numerical than the ones physically recorded, but the crest elevations matched or even slightly exceeded the predicted values. Furthermore, the rogue wave height did reduce over the 1.4 m recording distance and in fact dropped below the $H_{max}/H_s > 2.0$ criterion once it reached the final wave probe.
4. Overall, the design rogue wave model is suitable for hydrodynamic model testing of extreme wave impacts and air gap problems [5]; however, it is recommended to place the target crest as close to the wavemaker as practical since the generated rogue waves lost height and energy as they propagated (as mentioned above). Future development into obtaining target wave heights at locations further away from the wavemaker, through control of phase angles to focus wave energy precisely, would be valuable for model testing of platforms/vessels in realistic sea conditions.
5. Comparing rogue wave results between the 0.6 m and 0.7 m water depth tests, the greater water depth resulted in more consistent percentage differences in maximum wave height and showed close agreement with the target waves. Generating rogue waves in greater water depths than those tested in this work could potentially lead to more stable signals that allow for larger extreme waves to be modelled. However, further work is required to fully understand this effect.

Please cite this article as: B. Groves and N. Abdussamie, Generation of rogue waves at model scale, Journal of Ocean Engineering and Science, https://doi.org/10.1016/j.joes.2019.02.001

Acknowledgements

The authors would like to thank the Australian Maritime College for the use of the Model Test Basin facility, and its staff for the knowledge and support during testing.

References

[1] L. Bertotti, L. Cavaleri, Ocean Eng. 35 (1) (2008) 1–5.
[2] E. Bitner-Gregersen, O. Gramstad, Rogue waves impact on ships and offshore structures, DNV GL Strategic research & Innovation position paper, 2015, pp. 05–2015. DNV.GL.
[3] R. van Dijk, H. van den Boom, in: Proceedings of the ASME 2007 Twenty-sixth International Conference on Offshore Mechanics and Arctic Engineering, American Society of Mechanical Engineers, 2007.
[4] M. Christou, K. Ewans, J. Phys. Oceanograp. 44 (9) (2014) 2317–2335.
[5] S. Haver, Marine Struct. 63 (2019) 406–428.
[6] D. Walker, P. Taylor, R.E. Taylor, Appl. Ocean Res. 26 (3–4) (2004) 73–83.
[7] Haver, S. in *Rogue waves*. 2004.
[8] DNV, Recommended Practice DNV-RP-C205: environmental conditions and environmental loads. 2010: Norway.
[9] M. Li, J.-J. Shui, T. Xu, Appl. Math. Lett. 83 (2018) 110–115.
[10] M. Tong, D. Yevick, Wave Motion 66 (2016) 56–67.
[11] X.-B. Wang, T.-T. Zhang, M.-J. Dong, Appl. Math. Lett. 86 (2018) 298–304.
[12] K. Dysthe, H.E. Krogstad, P. Müller, Annu. Rev. Fluid Mech. 40 (2008) 287–310.
[13] Ransley, E.J., Survivability of wave energy converter and mooring coupled system using CFD. 2015.
[14] D. Ning, J. Zang, S. Liu, R.E. Taylor, B. Teng, P. Taylor, Ocean Eng. 36 (15–16) (2009) 1226–1243.
[15] T. Adcock, P. Taylor, S. Yan, Q. Ma, P. Janssen, in: Proceedings of the Royal Society of London A: Mathematical, Physical and Engineering Sciences, The Royal Society, 2011.
[16] T.B. Benjamin, J. Feir, J. Fluid Mech. 27 (3) (1967) 417–430.
[17] D.F. Gunn, M Rudman, R.C. Cohen, A. Chabchoub, in: The Twenty-fifth International Ocean and Polar Engineering Conference, International Society of Offshore and Polar Engineers, 2015.
[18] A. Chabchoub, N. Hoffmann, N. Akhmediev, Phys. Rev. Lett. 106 (20) (2011) 204502.
[19] F. Fedele, J. Brennan, S.P. De León, J. Dudley, F. Dias, Sci. Rep. 6 (2016) 27715.
[20] M. Banks, N. Abdussamie, J. Ocean Eng. Sci. 2 (3) (2017) 161–171.
[21] N. Gao, Y. Yang, W. Zhao, X. Li, Ships Offshore Struct. 11 (8) (2016) 802–817.
[22] N. Abdussamie, Y. Drobyshevski, R. Ojeda, G. Thomas, W. Amin, Ocean Eng. 142 (2017) 541–562.
[23] A. Chabchoub, H. Hoffmann, M. Onorato, N. Akhmediev, Phys. Rev. X 2 (1) (2012) 011015.
[24] Y. Deng, Y. Yang, X. Tian, X. Li, L. Xiao, Ocean Eng 118 (2016) 83–92.

Please cite this article as: B. Groves and N. Abdussamie, Generation of rogue waves at model scale, Journal of Ocean Engineering and Science, https://doi.org/10.1016/j.joes.2019.02.001